AIAA JOURNAL
Vol. 30, No. 9, September 1992

Mixing Studies of Helium in Air at High Supersonic Speeds

E. J. Fuller,* R. B. Mays,* R. H. Thomas,† and J. A. Schetz‡
Virginia Polytechnic Institute and State University, Blacksburg, Virginia 24061

This paper presents a mixing study using gas injection at low transverse angles into $M = 3$ and $M = 6$ crossflows. Effects of injectant asymmetries on the mixing processes were also tested by including low injector yaw angles. Ambient temperature helium was injected at matched pressure conditions as well as at 5 × matched pressure into a Mach 6 freestream, with Reynolds number of 5.4×10^7/m. Complementary tests at Mach 3, $Re = 5.0 \times 10^7$/m, were performed. The primary data are concentration measurements and meanflow measurements with nanosecond exposure shadowgraphs and surface flow visualization. At Mach 6, the matched pressure injection case, as compared to the underexpanded case, was found to show a greater injectant core penetration growth rate and a greater concentration decay rate. When the Mach 6 results were compared to similar experiments with a Mach 3 freestream, only a small decrease in the downstream core penetration and mixing rates was observed. However, due to much less initial mixing near the injector at the higher Mach number, the Mach 6 results showed a longer distance for the injectant core to decay to a concentration level corresponding to the H_2-air stoichiometric ratio. Other results showed that the plume remained supersonic and that moderate total pressure losses were found. Also observed was that, for both Mach 3 and Mach 6 freestreams, injector yaw did not increase the rate of decay of the maximum concentration, but that yaw did cause an increase in the overall injectant plume cross section, thus increasing the size of the mixing region.

Nomenclature

A_α	= area inside a given helium concentration contour
d	= diameter of the jet throat
P_c	= cone-static pressure
P_{eb}	= effective back pressure
P_{tp}	= total pressure parameter
V_o	= output voltage
x	= axial distance downstream of the injector
$(x/d)_{st}$	= mixing length to stoichiometric ratio
y	= lateral distance from the leading edge of injector
z	= vertical distance from test plate
z_{max}	= vertical location of α_{max}
α_{He}	= helium mass fraction concentration
α_{max}	= maximum helium mass fraction at an axial measurement station
β	= yaw angle of the injector
η_1	= penetration rate of the helium core
η_2	= decay rate of the helium concentration
θ	= transverse injection angle

Subscripts

j	= jet property
mix	= mixture property
p	= property inside the concentration probe
1	= local property
2	= post normal shock local property
∞	= freestream property

Introduction

GASEOUS injection into supersonic streams has a number of practical applications. One prominent example is fuel injection in the combustor of an aerospace plane. The National Aerospace Plane (NASP) program aims to develop a new generation of air-breathing aerospace vehicles for the aeronautics, space, and defense programs. High-speed, air-breathing ramjet performance can be increased if the combustion is allowed to take place supersonically, i.e., supersonic combustion ramjet.[1] Because of scramjet engine combustor velocities in the order of 3000 m/s, residence times of fuel in the combustor[2] are on the order of 10^{-3} to 10^{-4} s. Thus, supersonic mixing rates must be increased to maximize the heat release with the given combustor length constraint.[3] At the same time, total pressure losses must be minimized. This research addresses the simulated mixing of fuel and air, using a nonreacting case, at Mach numbers of 3 and 6.

An overview and analysis of high-speed mixing experiments, from normal injection to angled injection, can be found in Ref. 4. Gaseous injection, normal to a supersonic airflow, is one of the most studied cases. Experimental data on normal injection was collected by Rogers with single normal injectors[5] and arrays of normal injectors[6] into a supersonic crossflow. It was found that the normal injection scheme caused large total pressure losses and a decrease in mixing rate

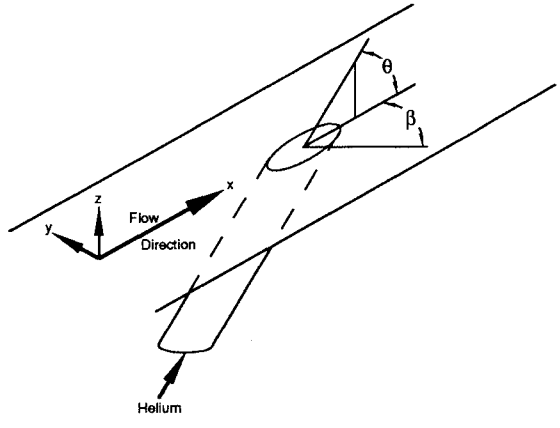

Fig. 1 Injector geometry and coordinate system.

Presented as Paper 91-2268 at the AIAA/SAE/ASME/ASCE 27th Joint Propulsion Conference, Sacramento, CA, June 24-26, 1991; received Aug. 15, 1991; revision received Jan. 31, 1992; accepted for publication Feb. 4, 1992.

*Graduate Student, Department of Aerospace and Ocean Engineering. Student Member AIAA.
†Research Associate, Department of Aerospace and Ocean Engineering. Member AIAA.
‡W. Martin Johnson Professor and Department Head, Department of Aerospace and Ocean Engineering. Fellow AIAA.

as the injector spacing was decreased. Another disadvantage to normal injection is the loss of any injectant thrust contribution that is important at high Mach numbers. In an attempt to capture all of the injectant thrust, studies were conducted by Hyde et al.,[7] Kwok et al.,[8] and others using a downstream facing slot. Results from these studies showed that the total pressure loss was small, but that the injectant mixing and penetration rates were also small. King et al.[9] conducted a study in which the downstream facing slot was coupled with an array of normal injectors and found that, with this scheme, large eddies were formed that entrained significant amounts of freestream air. Thus, the mixing was better than in the case of slot injection alone.

A second compromise between normal and slot injection into a supersonic flow was studied by McClinton[10] and Mays et al.[11] who chose to angle the injection jets downstream. McClinton studied arrays of closely spaced sonic injectors at constant dynamic pressure for transverse angles of 30, 45, 60, and 90 deg. Results from his studies showed that total pressure loss decreased while penetration and mixing increased as the injection angle was decreased. Mays et al. extended the work of McClinton by studying gaseous injection through a single, sonic nozzle with low transverse angles of 15 and 30 deg. When total pressure losses were considered, Mays et al. concluded that the 5 × matched pressure, 15-deg transverse angled injection case was the best.

Recent studies into turbulent flow separation control at subsonic speeds have demonstrated that skewed vortex generator jets (VGJ) show promise in helping to delay or eliminate stall. Johnston and Nishi[12] demonstrate that, in low-speed airflow experiments, the VGJ method creates longitudinal vortices in the boundary layer that, through cross-stream mixing of streamwise momentum, are effective in the reduction and elimination of stalled regions. Lin et al.[13] show that the vortices energize the low-energy boundary-layer flow through a three-dimensional process. The experiments presented in this paper attempted to use a skewed injector in order to energize the injectant plume and increase mixing.

Presented here are the results from experiments designed to further expand the data base of gaseous injection into supersonic crossflows. These studies were performed at both Mach 6 and Mach 3. Included in these studies are several cases of gaseous injection with low transverse angles into a Mach 6 freestream, as well as injection with low transverse angles coupled with a low yaw angle. From the previous work with VGJs, it was believed that gaseous injection into a supersonic freestream with a low transverse angle as well as a low yaw angle could increase the injectant mixing rate. Also believed was that plume spreading could be increased through a three-dimensional vortical interaction. With low transverse and yaw angles, the majority of the injectant thrust is retained. Ambient temperature helium was used in these tests, for safety reasons, to simulate hydrogen injection. These tests, conducted at NASA Langley Research Center, were the first mixing studies of this type to be conducted at a high Mach number ($M > 4$), which better simulates the conditions existing in a scramjet combustor of a vehicle traveling at high flight Mach numbers, $M_\infty \approx 15$–20.

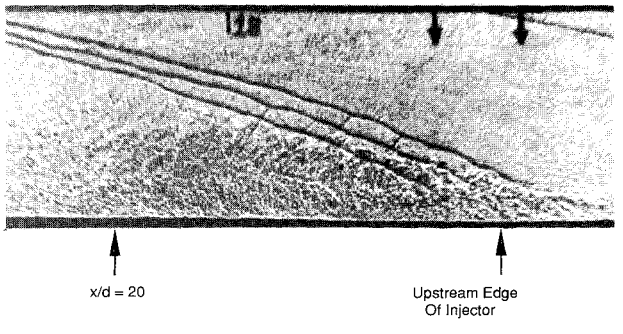

Fig. 2 Mach 6, $\theta = 15$ deg, $\beta = -15$ deg, $P_j/P_{eb} = 5$.

Test Facilities

The NASA Langley facility used was the Mach 6 high Reynolds number tunnel with a 30.5-cm-diam straight test section. The tunnel conditions were set such that a freestream Reynolds number of 5.4×10^7/m was achieved. The facility used at Virginia Polytechnic Institute consisted of a 23 × 23 cm Mach 3 blowdown supersonic tunnel. Again, conditions were set to obtain a freestream Reynolds number of 5.0×10^7/m. The Virginia Tech test section was 11.5 cm high by 23 cm wide and more than 30 cm in the streamwise direction. Data acquisition for both facilities consisted of an AT computer with a 16 channel, 12 bit A/D board.

Assuming a hypersonic cruise flight vehicle with an inlet Mach number diffusion ratio of 3, the tunnel conditions at Virginia Tech would simulate a vehicle with a flight Mach number of 9 at an altitude of 58 km. The freestream conditions in the NASA Langley tunnel would simulate a vehicle with a flight Mach number of 18 at an altitude of 73 km, which better models a true hypervelocity vehicle. Unfortunately, it was not possible in either test to simulate the high total temperatures or combustion that would be found in the combustor section of an actual scramjet. Even with these limitations, these facilities were able to successfully provide the conditions needed to establish the mixing trends.

Models

The NASA Langley model was a flat plate 99.1 cm long by 19.7 cm wide, which was supported by a strut on either side, running the length of the model. A circular nozzle block contained three injectors and was located such that the upstream edge of the injectors, in the unyawed configuration, was 35.6 cm from the leading edge. The three injectors each had a throat diameter of 0.635 cm, followed by a conical expansion to produce a helium jet Mach number M_j of 1.7 at the injector exit. The injectors were spaced at $9.0d$ and were designed to have a 15-deg downstream transverse angle. Yaw angles of 0 and −15 deg were introduced by rotating the nozzle block.

The model used for the Virginia Tech studies consisted of a single injector located at the center of a circular nozzle block. This nozzle block was mounted flush with the flat centerline wall of a half nozzle and was able to rotate from $\beta = 0$ to −28 deg. The origin of the right-hand coordinate system was located at the upstream edge of the injector with positive x in the streamwise direction. The helium injector selected was the 30-deg downstream angled sonic injector studied by Mays et al.[11] with a converging section to a 0.318-cm-diam exit. The other helium injector used by Mays et al.[11] was a single, sonic helium injector with a 15-deg transverse angle with injector geometry similar to the 30-deg injector. Figure 1 illustrates the injector geometry and coordinate system used for both sets of experiments.

Test Matrix

The analysis of Schetz and Billig[14] on 90-deg jets included the introduction of the effective back pressure concept. This effective back pressure P_{eb} was defined as the average pressure

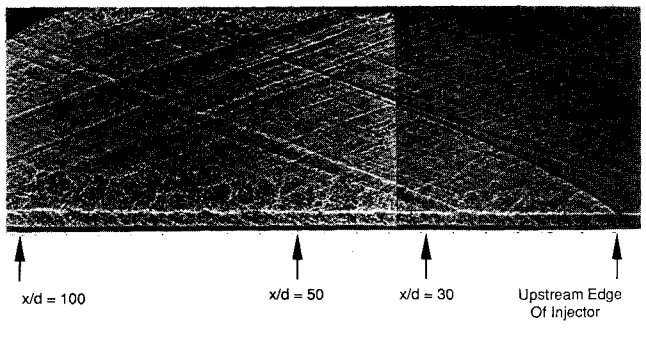

Fig. 3 Mach 3, $\theta = 30$ deg, $\beta = -28$ deg, $P_j/P_{eb} = 5$.

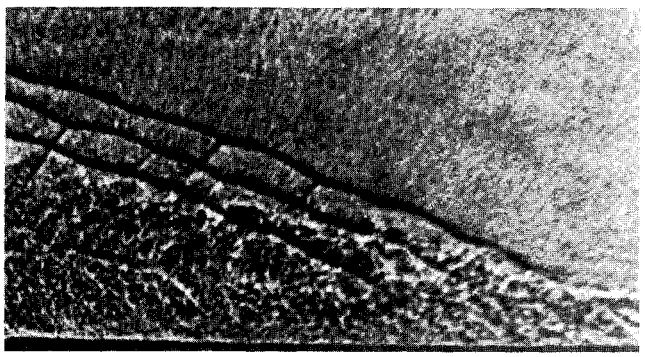

Fig. 4 Mach 6, $\theta = 15$ deg, $\beta = -15$ deg, $P_j/P_{eb} = 5$ (blow up).

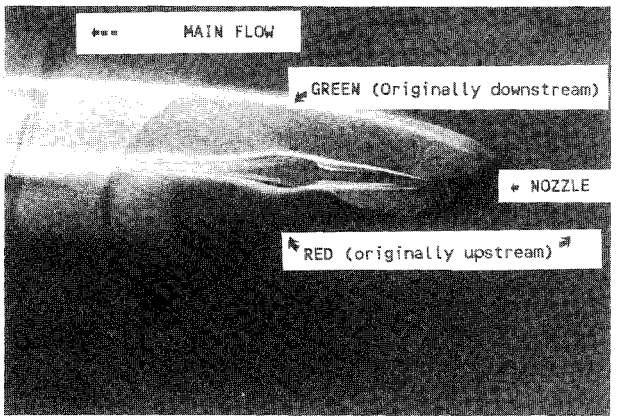

Fig. 5 Mach 3, $\theta = 30$ deg, $\beta = -28$ deg, $P_j/P_{eb} = 5$.

between the jet interaction shock and the jet itself. P_{eb} can also be defined by the pressure to which the jet will expand after leaving the injector. The current low-angled jet was crudely modeled as a cone with a cone half-angle equal to the injection angle. For a given freestream Mach number and pressure, the static pressure on the cone could be calculated, and this was assumed to be equal to P_{eb}. From this notion of an effective back pressure, an expansion ratio can be defined as the ratio of the static jet pressure at the orifice to the effective back pressure. An underexpansion ratio is indicated by an expansion ratio greater than 1.

The previous studies by Mays et al.,[11] involving both matched pressure and 5 × matched pressure (5 × underexpanded), low transverse angle injection, at Mach 3, showed that 5 × underexpanded helium injection schemes have significantly better mixing and penetration rates as compared to matched pressure injection. The NASA experiments were performed with both matched pressure and 5 × underexpanded injection in order to observe the trends in a Mach 6 freestream. The Mach 3 Virginia Tech yawed injection experiments were performed at a 5 × injectant underexpansion ratio.

Tests were performed with $\beta = 0$ and -15 deg at both Virginia Tech and NASA. An additional $\beta = -28$ deg case was tested at Virginia Tech. For each of these tests, concentration, as well as meanflow measurements, were taken at several downstream axial stations. Meanflow measurements consisted of pitot pressure, total temperature, and cone-static pressure measurements. In the Virginia Tech facility, at each axial station, lateral stations were located from -5 to $5d$ in increments of $1d$, and continuous vertical traverses were made at each lateral location. At NASA, point measurements were made with a vertical spacing of $0.5d$, thus giving a grid of 1–$0.5d$, y to z, respectively. The axial locations for the Virginia Tech tests were 30, 50, and $100d$. For the NASA tests, the axial locations were 20, 40, 60, and $80d$. Because of space constraints, only selected results will be presented here.

Concentration Measurements

Helium concentration measurements were made for both test series using an aspirating hot-film concentration probe based on the original design of Ng et al.[15] Data required to determine concentration consist of the hot-film voltage, total pressure, and the total temperature of the flow at the sensor. Total pressure and temperature were measured in the probe, just upstream of the sensor location, where the Mach number was very low. A choked orifice, behind the sensor, allowed for the massflow past the sensor to be calculated with the measured pressure and temperature. A separate calibration facility was used to generate the curves relating the hot-film voltage, pressure, and temperature to a known helium concentration. For the tests at Virginia Tech, it was only necessary to calibrate at room temperature, but at NASA Langley, due to the higher temperatures involved, the rig was designed to calibrate at temperatures ranging from room temperature to 540 K.

The probe geometry differed from Virginia Tech to NASA Langley. For the tests conducted at Virginia Tech, the hot film was mounted approximately 2 cm from the inlet. This resulted in low flush times and allowed for a continuous vertical traverse of 0.4 cm/s while the data was taken at 100 Hz. At NASA Langley, due to the high tunnel temperature and possible blockage from the probe and traversing mechanism, the sensor was mounted approximately 60 cm behind the inlet, requiring a point to point measurement scheme. The probe was traversed to the desired point and allowed to flush for 0.75 s before the data was taken at 100 Hz for 0.25 s.

Meanflow Measurements

A meanflow rake, containing a pitot probe, total temperature probe, and a 10-deg half-angle cone-static pressure probe, was designed and manufactured for use in the NASA Langley Mach 6 high Reynolds number tunnel. This rake was mounted on a strut that was connected to the traversing mechanism and extended downward into the freestream. During a run, the rake was moved to a known location, the probes allowed to flush for 0.75 s, then the data were taken. Once the data were taken, the rake was moved and the process repeated. Lateral movements were set equal to the known probe spacing, thus allowing identical vertical slices to be measured by each probe. With this rake and traversing mechanism, all three meanflow quantities could be measured at identical locations during the same run. Each meanflow quantity had to be measured during different runs at Virginia Tech. During each run, a single probe made one upward traverse, with the speed set slow enough so as to minimize any lags in the data.

Data Reduction

The data reduction process was divided into two parts—the concentration data reduction followed by the mean flow data reduction. The concentration data reduction used the calibration curves to convert the hot-film voltages P_p and T_p to a helium mole fraction value. The resulting concentrations were then converted to mass fractions and used in the mean flow data reduction to calculate Mach number, density, velocity, and mass flux distributions. The mean flow data reduction was more routine in that it utilized standard flow equations to retrieve the final quantities.

Concentration Data Reduction

Concentration probe hot-film voltage is related to the Reynolds number by Eq. (1), where R_s, R_w, l, and T_w were known, k was a function of the gas composition, and T_t was measured at the sensor location. Constants a, b, and m were determined by the concentration probe calibration:

$$V^2 = \frac{(R_s + R_w)^2}{R_w} \pi l k (aRe^m + b)(T_w - T_t) \tag{1}$$

For each vertical traverse, a file was generated containing the probe location, sensor voltage, probe pressure, and probe

total temperature. At each point, the program would use Eq. (1) with P_p and T_p to calculate the upper and lower voltage bounds at given calibrated levels. The program would then start with the calibration curve of the lowest helium concentration and sequentially search for the two curves that bounded the voltage at the appropriate pressure. The helium concentrations of the bounding curves were used to interpolate for the experimental concentration. Contour plots were generated for each axial station by assembling and interpolating reduced data from all of the lateral stations.

Meanflow Data Reduction

A FORTRAN program used the previously calculated helium concentration data, the cone-static pressure, pitot pressure, and total temperature data to calculate profiles of Mach number, velocity, mass flux, as well as the static density, pressure, and temperature in the flowfield. Values of γ and R were computed according to the helium concentration at each location. The Mach number was calculated using the cone-flow and Rayleigh-pitot equations. The static pressure dependence was eliminated by combining these two equations, making P_c/P_{t2} a function of M_1 and γ. This relationship was used to generate a table of Mach numbers as a function of γ and the ratio P_c/P_{t2} for a 10-deg half-angle cone. Using this table and the Rayleigh-pitot formula, the Mach number and static pressure were calculated at each datum point. With the Mach number now known, and utilizing the fact that $T_{t2} = T_{t1}$ across a shock, the program then calculated the static temperature from the isentropic temperature relation. The local speed of sound, velocity, and density were then calculated by use of the perfect gas equations.

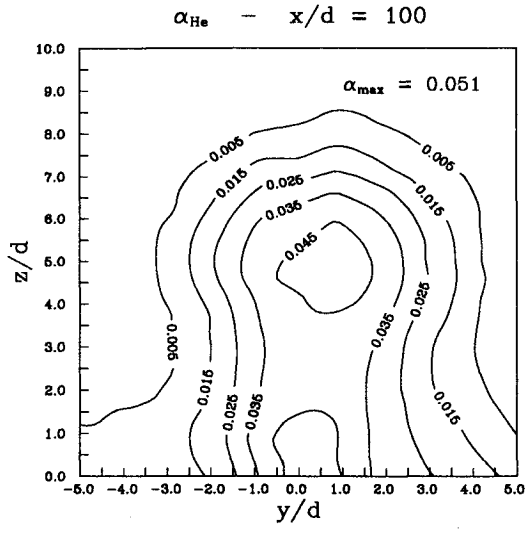

Fig. 6 α_{He}: Mach 3, $\theta = 30$ deg, $\beta = 0$, $x/d = 100$.

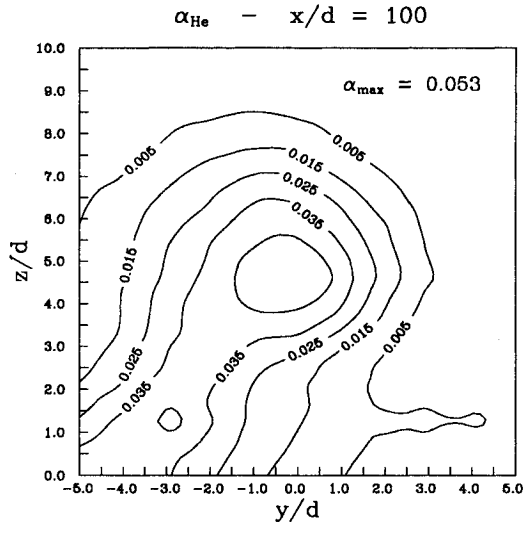

Fig. 7 α_{He}: Mach 3, $\theta = 30$ deg, $\beta = -28$, $x/d = 100$.

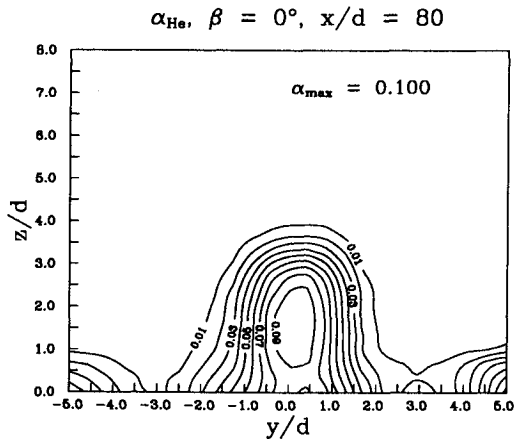

Fig. 8 α_{He}: Mach 6, $\theta = 15$ deg, $\beta = 0$ deg, $x/d = 80$.

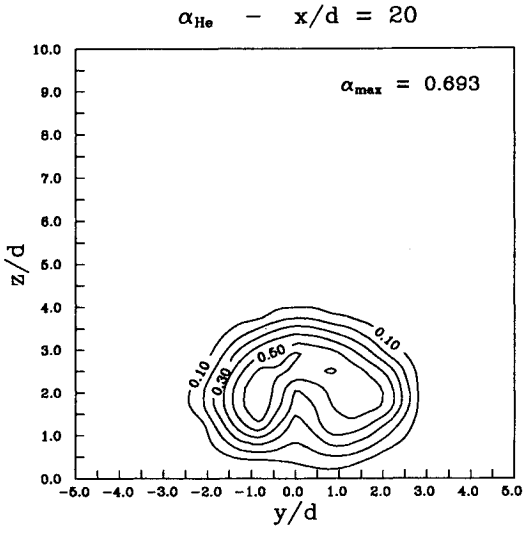

Fig. 9 α_{He}: Mach 6, $\theta = 15$ deg, $\beta = 0$ deg, $x/d = 20$.

Mass flux at a location was calculated by multiplying the local density by the velocity at that point. Total pressure was calculated from the pitot pressure by using the normal shock equation. Probe locations were then nondimensionalized by the jet throat diameter, and all other quantities were nondimensionalized by their respective freestream values.

Results

Shadowgraphs

Ten nanosecond (2×10^{-8} sec) exposure time shadowgraphs (nanoshadowgraphs) were made for most of the injection cases. In 2×10^{-8} s, a particle will only travel 6.2×10^{-3} mm in the Virginia Tech tunnel and only 9.6×10^{-3} mm in the NASA Langley tunnel. Therefore, with exposure times this small, the flowfield, including the turbulent eddies, could be stopped.

Figure 2 is an example of a nanoshadowgraph taken during the tests performed at NASA Langley at Mach 6, $\theta = 15$ deg with the injectant 5 × underexpanded. The flow direction is from right to left. The incoming boundary layer can be seen, as well as the injectant bow shocks and the injectant itself. Although gradients in refractive index are produced in this

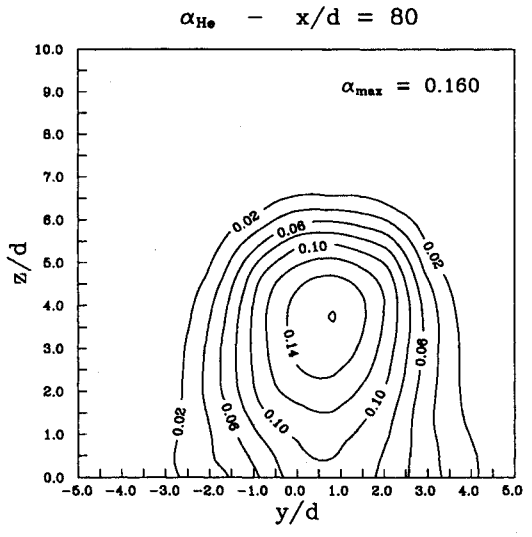

Fig. 10 α_{He}: Mach 6, $\theta = 15$ deg, $\beta = 0$ deg, $x/d = 80$.

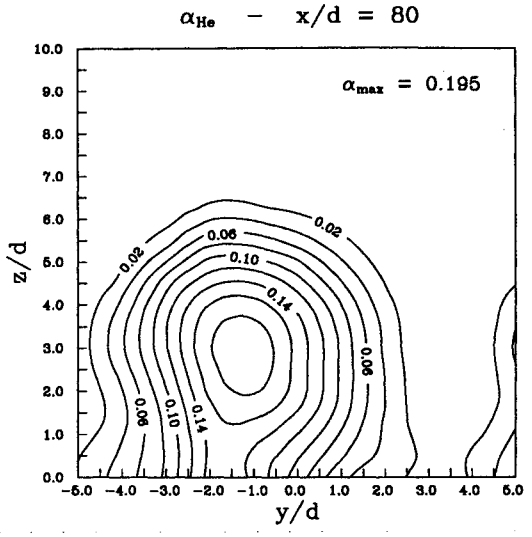

Fig. 12 α_{He}: Mach 6, $\theta = 15$ deg, $\beta = -15$ deg, $x/d = 80$.

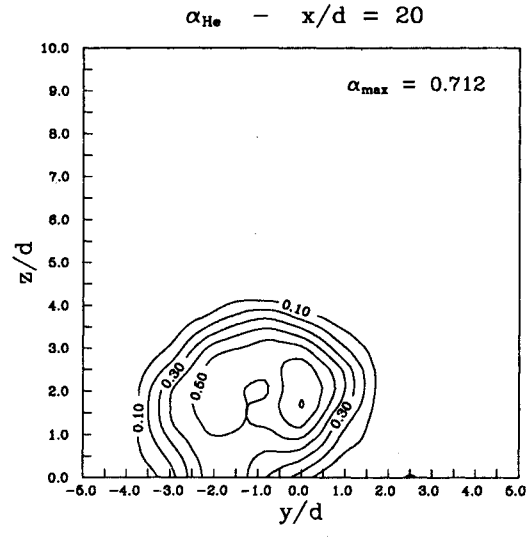

Fig. 11 α_{He}: Mach 6, $\theta = 15$ deg, $\beta = -15$ deg, $x/d = 20$.

flow both by density gradients in the flow and species concentration gradients between the He and air, the primary source of these gradients is the injectant plume. All three bow shocks can be clearly seen due to the fact that for this picture the nozzle block was yawed 15 deg, thus moving the farthest injector upstream and the nearest injector downstream. The boundary layer is measured to be approximately $1d$ at the leading edge of the injectors. After approximately $10d$ downstream of the injectant entry, the boundary layer becomes less distinct, and by $x/d \approx 20$, one cannot distinguish the boundary layer from the injectant. Most important, large-scale eddies in the injectant, which are vital for initial significant entrainment, can be seen in Fig. 2. Because this shadowgraph is an integration across all three injectors, the large eddies, which are known to exist in each plume, are not distinct, preventing good eddy size measurements.

Figure 3 is an example of a nanoshadowgraph taken during the Virginia Tech Mach 3, $\theta = 30$ deg, 5× underexpanded injection tests. This particular nanoshadowgraph was taken with $\beta = -28$ deg. Again, injection occurs at the far right of the picture with the arrow indicating the upstream edge of the injector. The wall boundary layer, containing turbulent eddies, can be seen clearly as it is bounded by the wall and a white band. At the injector, the boundary-layer thickness is measured to be approximately $1.6d$ and grows to approximately $2.0d$ by the last measurement station. The measurement stations are indicated on the picture. Large scale eddies can also be seen in the injectant plume. From measurements on the picture, it can be seen that these large eddies are approximately $2d$ in size at $x/d = 30$, and by $x/d = 100$, they grow to a size of approximately $4d$.

In Fig. 4, a blow up of the near injector region of Fig. 2, the bow shocks can be seen to be very close to the jet, and most important, it can be seen to be unsteady. This unsteadiness can be observed from the fact that the bow shocks are kinked. Associated with each kink are waves orthogonal to the main bow shock. Fuller et al.[17] showed that these kinks and orthogonal waves (orthowaves) appear to become more pronounced as the injector yaw angle is increased. As was the case with the kinks and orthowaves, the eddies in the injectant plume also appear to become somewhat larger and more distinct as the yaw angle is increased. From this observation, it appears that the eddies are related to the kinks and orthowaves, thus freestream entrainment may be related to the injectant bow shock unsteadiness.

Surface Flow Visualization

Surface flow experiments were performed at both NASA Langley and Virginia Tech using fluorescent dye mixed in a silicone oil of 500 cS. The oil was illuminated with ultraviolet lights. Still color photographs were taken at Virginia Tech, and video tape recordings were made during the tests at NASA Langley. Figure 5 is an oil flow picture showing the near field for a yaw angle β of -28 deg from a skewed, downward angle. The freestream is from right to left, thus the injector is venting to the left. Because of the coordinate system used, the positive y direction is toward the bottom of the pictures. It can be seen in Fig. 5 that at a yaw angle of -28 deg large asymmetries appeared. The diamond pattern that can be seen just aft of the injector was observed for all cases and appeared to remain unchanged. The asymmetries appear outside the diamond in that flow on the $+y$ side wraps around the jet, indicating freestream mixing just off the floor, whereas on the $-y$ side, there appears to be little mixing of the freestream near the floor. This asymmetry grew stronger as β was increased.

Concentration Field Data

The sets of vertical profiles at a given axial location were processed to give lateral contour plots, as seen in Figs. 6–12. Because the coordinate system was defined in Fig. 1, these contour plots are shown as if the helium jet were coming out of the page. Key information that can be seen in these plots are the location and approximate maximum mass fraction value of the injectant core, as well as the overall penetration and

Table 1 Mach 6 helium concentration penetration and mixing results

Case	x/d	α_{max}	z_{max}/d	η_1	η_2	$(x/d)_{st}$
$M = 6$	20	0.695	0.0			
$\theta = 15$ deg	40	0.286	0.2			
$\beta = 0$ deg	60	0.136	1.3	1.23	1.43	181.7
$P_j/P_{eb} = 1$	80	0.100	1.6			
$\bar{q} = 0.48$						
$M = 6$	20	0.737	0.0			
$\theta = 15$ deg	40	0.421	0.2			
$\beta = -15$ deg	60	0.165	1.3	1.03	1.40	213.4
$P_j/P_{eb} = 1$	80	0.113	1.4			
$\bar{q} = 0.48$						
$M = 6$	20	0.693	2.6			
$\theta = 15$ deg	40	0.401	2.8			
$\beta = 0$ deg	60	0.215	3.0	0.64	1.08	397.7
$P_j/P_{eb} = 5$	80	0.160	3.6			
$\bar{q} = 2.35$						
$M = 6$	20	0.712	2.1			
$\theta = 15$ deg	40	0.465	2.6			
$\beta = -15$ deg	60	0.332	2.7	0.59	0.88	815.0
$P_j/P_{eb} = 5$	80	0.195	3.0			
$\bar{q} = 2.35$						
$M = 6$	20	0.568	2.0			
$\theta = 15$ deg	40	0.314	2.8			
$\beta = 0$ deg	60	0.169	3.2	1.08	1.13	287.4
$P_j/P_{eb} = 5$	80	0.120	3.5			
B.L. Trips						

Table 2 Mach 3 helium concentration penetration and mixing results

Case	x/d	α_{max}	z_{max}/d	η_1	η_2	$(x/d)_{st}$
$M = 3$	30	0.379	3.3			
$\theta = 30$ deg	50	0.124	3.9			
$\beta = 0$ deg	100	0.051	5.0	1.42	1.64	133.5
$P_j/P_{eb} = 5$						
$\bar{q} = 3.11$						
$M = 3$	30	0.397	3.2			
$\theta = 30$ deg	50	0.131	3.8			
$\beta = -15$ deg	100	0.048	4.1	0.73	1.74	128.2
$P_j/P_{eb} = 5$						
$\bar{q} = 3.11$						
$M = 3$	30	0.378	3.2			
$\theta = 30$ deg	50	0.128	3.5			
$\beta = -28$ deg	100	0.053	4.6	1.19	1.61	138.0
$P_j/P_{eb} = 5$						
$\bar{q} = 3.11$						
$M = 3$	20	0.20	0.25			
$\theta = 15$ deg	40	0.10	0.90			
$\beta = 0$ deg	90	0.05	1.55	0.86	0.92	157.5
$P_j/P_{eb} = 1$						
$\bar{q} = 0.27$						
$M = 3$	20	0.30	2.05			
$\theta = 15$ deg	40	0.10	2.70			
$\beta = 0$ deg	90	0.05	3.85	1.20	1.18	132.4
$P_j/P_{eb} = 5$						
$\bar{q} = 1.37$						

spreading of the jet. From the vertical location and the mass fraction value of the injectant core, core decay rates η_2, defined as the rate at which the helium core concentration decreases assuming $\alpha_{max} = \xi_2^*(x/d)^{-\eta_2}$, and core penetration growth rates η_1, defined as the rate at which the helium core travels upward, assuming $(z_{max}/d) = \eta_1 \log(x/d) + \xi_1$, can be determined for each case. Injectant core penetration rates in the boundary layer are different as compared to when the injectant core has penetrated into the freestream; however, due to lack of data very near the injector, this has been neglected for this penetration model. After the maximum concentration decay rates were calculated, it was possible to calculate the distance for the entire plume to decay to a concentration level equal to or below that of the H_2-air stoichiometric. This distance, the H_2-air stoichiometric ratio $(x/d)_{st}$, is defined as the streamwise distance required for the injectant core to decay to the H_2-air stoichiometric ratio of 0.029. The H_2-air stoichiometric ratio was chosen to be merely a point of reference, and it is not implied that $(x/d)_{st}$ is the location where combustion will be complete, but $(x/d)_{st}$ is an important factor in that it is related to a required scramjet combustor length. Tables 1 and 2 summarize the results of the NASA Langley Mach 6 and the Virginia Tech Mach 3 experiments, respectively.

Mays et al.[11] reported that, in the Mach 3, $\theta = 15$ deg, $\beta = 0$ deg injection experiments, as the injectant underexpansion ratio was raised from 1 to 5, the core penetration growth rate η_1 increased 40% and the maximum concentration decay rate η_2 increased 28%. This corresponded to an $(x/d)_{st}$ decrease of 16%. Also observed was that the core penetrated much farther into the freestream in the 5 × underexpansion case. One finds it interesting to note that these trends did not hold true when the new mixing studies were conducted at Mach 6. Table 1 shows that at Mach 6, $\theta = 15$ deg, $\beta = 0$ deg, when the injectant underexpansion ratio was increased from 1 to 5, η_1 decreased 48% and η_2 decreased 24%, corresponding to an $(x/d)_{st}$ increase of 119%. However, the absolute core penetration was much less for the case of matched pressure injection, in that at $x/d = 80$, the injectant core vertical location for the matched pressure case was less than half the value for the 5 × underexpanded case. This is most likely due to the fact that for the underexpanded case, the injectant penetrates the boundary layer much quicker than for the matched pressure case. Once outside the boundary layer, the injectant is swept downstream much faster and thus has less time to move upward and mix. Since the injectant in the matched pressure case remained in the boundary layer much longer than for the underexpanded case, there appears a larger penetration growth rate because of the steady upward movement of the injectant. Prolonged times for boundary-layer penetration also make the core decay rate greater for the matched pressure case. This is due to the increased time for the injectant to travel the test distance and the higher turbulence levels in the boundary layer combining to increase the mixing rate.

To support this theory, an experiment was run at NASA Langley where the incoming boundary layer was thickened by a factor of approximately 1.5. This was achieved by normal injection of air, through an array of very small injectors just aft of the model leading edge. Table 1 illustrates that, with a thicker boundary-layer, core penetration rates and decay rates increased for the case of an injectant 5 × underexpansion ratio over the case of the original boundary-layer thickness. η_1 was observed to increase 68% and η_2 increase 5%. This resulted in a 28% decrease in $(x/d)_{st}$. There was very little difference observed in the absolute core penetration by $x/d = 80$ between the two cases.

A comparison between similar injector conditions for Mach 3 and Mach 6 shows that, for matched pressure injection, the core penetration growth and concentration decay rates increase in going from Mach 3 to Mach 6. The 15-deg injector conditions were not identical because the Mach 3 injector was sonic, whereas the Mach 6 injector was supersonic, $M_j = 1.7$. The incoming boundary-layer thicknesses were also different, $1.6d$ and $1.0d$ for Mach 3 and Mach 6, respectively. In comparing the case of an injectant underexpansion ratio of 5 ×, it is best to compare the Mach 3 data to the Mach 6 increased boundary-layer thickness case due to a better match of incoming boundary-layer thicknesses. In going from Mach 3 to

Mach 6, there is only a 5% decrease in η_2 and a 10% decrease in η_1. The distances to an H_2-air stoichiometric ratio were greater for both the matched pressure and underexpanded cases at Mach 6 in comparison to the Mach 3 values. This is due to the fact that the core concentration values were much higher for the experiments conducted at Mach 6, suggesting much lower initial mixing at Mach 6 as compared to Mach 3.

Because of a significant increase in the injectant mass flow as the underexpansion ratio is raised, an effective jet diameter d_{eff} was formulated by using the mass flow ratio of the injectant to freestream as follows:

$$d_{\text{eff}} = \sqrt{\frac{\rho_j u_j}{\rho_\infty u_\infty} d^2} \tag{2}$$

Figure 13 illustrates the core penetration for both Mach 3 and 6, $\theta = 15$ deg, $\beta = 0$ deg using the effective jet diameter. One can note that the matched pressure injection cases exhibit a greater penetration growth rate, but much less initial penetration, as compared to the 5 × underexpanded injection cases. Also found was that, when the boundary layer was thickened at Mach 6, the penetration growth rate increased significantly. Figure 14 presents the maximum concentration decay rates for both Mach 3 and 6, $\theta = 15$ deg, $\beta = 0$ deg. Using d_{eff} as the nondimensionalizing parameter has the effect of bringing the cases together in that the decay rates are nearly identical. Figure 14 shows that, when d_{eff} is used, matched pressure injection, at both Mach 3 and 6, exhibits less initial mixing and that the Mach 6 cases all show less initial mixing than the cases at Mach 3.

Tables 1 and 2 also demonstrate the effects of injector yaw angle on the injectant penetration and mixing rates. At Mach 3, $\theta = 30$ deg, when the injector yaw was increased from 0 to -28 deg, less than a 4% change in the maximum concentration decay rate was observed, but the rate of core penetration was significantly affected. At Mach 6, $\theta = 15$ deg, $\beta = -15$ deg, η_1 decreased by 16% and η_2 decreased by 2% for the case of matched pressure injection. For the case of 5× underexpanded injection, the core penetration rate decreased by 9% and rate of maximum concentration decay decreased by 19%. Thus, for the underexpanded cases, increasing the injector yaw angle has more effect on the core penetration and decay rates at Mach 6, $\theta = 15$ deg than at Mach 3, $\theta = 30$ deg.

The initial disturbance of injection at a transverse angle of 30 deg is believed to be great enough so that any added disturbance, e.g., coupling a yaw angle with the transverse angle, thus increasing the injectant frontal area, would not be significant enough to alter the mixing rate to any great degree. Whereas, with a transverse angle of 15 deg, the initial injectant frontal area is less, thus the initial disturbance is smaller than that for 30 deg transverse injection, so that by introducing injector yaw, the added disturbance from the increased frontal area becomes more significant. This increase in frontal area creates a stronger bow shock, causing a less energetic flowfield behind the shock, which would explain a decrease in the mixing rate thus increasing the mixing distance $(x/d)_{\text{st}}$. In addition, the tests conducted at NASA Langley were performed with a freestream Mach number of 6 vs the freestream Mach number of 3 at Virginia Tech, which would tend to make the disturbances due to injection greater. The effect of increasing the injectant underexpansion ratio would also tend to increase the injectant frontal area, thus creating a larger disturbance. This increase in frontal area would increase the magnitude of the added disturbance due to injector yaw. It follows then that the effects of yaw would be greater at a larger underexpansion ratio, which is what was observed during the NASA Langley Mach 6 experiments.

By coupling an injector yaw angle with a transverse angle, it was also hoped to create injectant asymmetries and larger lateral spreading of the injectant plume to promote better mixing. In order to observe the asymmetries and lateral spreading, one must look at a surface contour. Figures 6–12 are helium concentration surface contour plots. Figure 6 is a helium concentration contour plot generated from the Virginia Tech Mach 3, $\theta = 30$ deg, and $\beta = 0$ deg case. It can be seen that the primary core of the injectant is roughly 5.0 diameters off the floor and is nearly on the centerline. There also appears to be a lateral symmetry about the core centerline. Figure 7 was generated from the Virginia Tech Mach 3, $\theta = 30$ deg, and $\beta = -28$ deg case. Similar to the unyawed case, one can see that the primary core is approximately on the centerline and nearly 5.0 diameters off the floor. In both cases, a secondary core can be observed in the boundary layer, approximately 1.0 diameters off the floor. In the case with no injector yaw, this secondary core exists almost directly beneath the primary core, whereas in the case of -28-deg injector yaw, the secondary core has moved $-3d$ off the centerline. There can be noted a definite shear line at a vertical location of $2d$, which corresponds to the boundary-layer thickness. Helium that was immediately peeled off the injectant plume never escaped the boundary layer and formed this secondary core. Because this secondary core was in the boundary layer, it had a higher lateral to streamwise momentum ratio as compared to the helium that escaped into the freestream, and was thus able to move laterally much more than the primary core. This lateral movement of the secondary core caused a shearing effect on the injectant plume, which stretched the plume and created a larger mixing area.

Figures 8–12 present a few of the helium concentration results from the experiments conducted at Mach 6, $\theta = 15$ deg in the NASA Langley facility. Figure 8 presents the NASA Langley baseline case of matched pressure injection at a transverse angle of 15 deg and no injector yaw angle, at a streamwise location of $x/d = 80$. The core can be seen to be at approximately $z/d = 1.6$ and again the injectant plume is

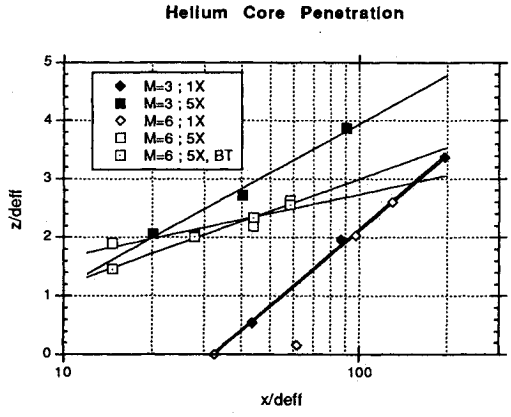

Fig. 13 Injectant core penetration.

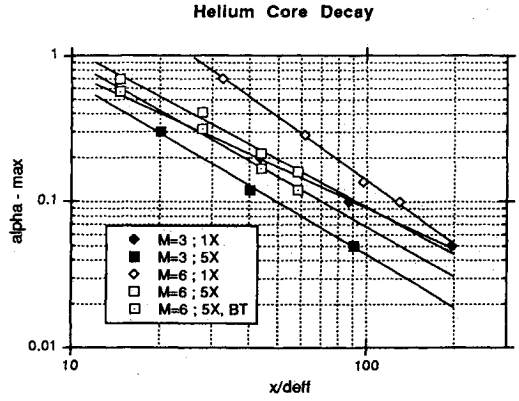

Fig. 14 Injectant core concentration decay.

Table 3 Total pressure parameters

Model conditions	β, deg	P_{tp}
Mach 3 $\theta = 30$ deg $P_j/P_{eb} = 5$	0 −28	0.54 0.53
Mach 6 $\theta = 15$ deg $P_j/P_{eb} = 1$	0 −15	0.69 0.70
Mach 6 $\theta = 15$ deg $P_j/P_{eb} = 5$	0 −15	0.49 0.51

roughly laterally symmetrical about the core. Figure 9 was generated from the results of the Mach 6, $\theta = 15$ deg, $\beta = 0$ deg, 5 × underexpanded injection test. This plot is at the closest axial station to the injector, $x/d = 20$, and clearly shows a kidney-shaped core. This kidney shape is most likely due to the symmetrical longitudinal vortices that are formed by the unyawed injectant plume. Again, there is lateral symmetry about the injectant centerline. By $x/d = 80$ in Fig. 10, the core has become roughly circular and risen to a vertical location of $z/d \approx 3.6$. Once more the injectant lateral symmetry is preserved. Figure 11, the Mach 6, $\theta = 15$ deg, $\beta = -15$ deg, and 5 × underexpanded injection case at $x/d = 20$, shows a loss of core symmetry in that the core is no longer shaped like a symmetrical kidney, but instead there appears to be a dominant side of the injectant plume, believed to be due to asymmetrical longitudinal vortices created by the injector yaw. Unfortunately, this desired asymmetry has disappeared by $x/d = 80$, Fig. 12. Figure 12 shows that the entire injectant plume has moved laterally with no apparent shearing. Because of the low transverse angle, $\theta = 15$ deg, lateral movement of the entire plume was possible due to the longer residence time of the injectant in the boundary layer. There was clear evidence of lateral spreading due to the lateral movement in that the area inside the α_{He} contour equal to 0.1 ($A_{\alpha=0.1}$) was measured for both the case of $\beta = 0$ and 15 deg. It was found that when $\beta = 0$ deg, $A_{\alpha=0.1} = 12.7d^2$, and when $\beta = 15$ deg, $A_{\alpha=0.1} = 17.6d^2$, which is clear evidence of lateral spreading leading to area growth of the injectant plume. At Mach 6, as the yaw angle was increased, no significant increase in representative areas were found in the matched pressure injection case, which tends to show that increasing the underexpansion ratio, at Mach 6, $\theta = 15$ deg, does increase the effectiveness of injector yaw on lateral spreading.

Meanflow Data

The data from the meanflow probe was reduced to give various flowfield data including the Mach number, total pressure, static pressure and temperature, and flow velocities. From this information, total pressure losses can be determined as well as other meaningful information. Control of the total pressure losses due to fuel injection is very important in a scramjet.

To compare the total pressure loss of each injection case, a nondimensional total pressure parameter (P_{tp}) was developed similar to the one presented in Ref. 11. Based on the suggestion of Ref. 11, the total pressure parameter was defined as follows:

$$P_{tp} = \frac{\int_{y_i}^{y_f}\int_{z_i}^{z_f} \rho u P_t dA}{\int_{y_i}^{y_f}\int_{z_i}^{z_f} \rho_\infty u_\infty P_{t\infty} dA + \rho_j u_j P_{tj} A_j} \qquad (3)$$

The first term in the denominator of Eq. (3) represents the total pressure of an undisturbed freestream boundary-layer flow. This was calculated by finding the volume below the surface of the mass weighted total pressure flux of the undisturbed approach flow. The second term in the denominator represents the injectant total pressure flux calculated from the stagnation properties of the jet, using the isentropic, perfect gas equations. The sum of these two terms represents the total pressure of the approach flow and the injectant, without any losses due to interactions between the two. The numerator of Eq. (3) represents the total pressure of the flow including the total pressure losses caused by the injectant-freestream interaction. This was calculated by determining the volume below the mass weighted total pressure flux surface, measured by a meanflow traverse at the last axial station for each injection case. The ratio of the numerator and denominator of Eq. (3) represents the total pressure of the actual field relative to the total pressure of the freestream-injector combination. Any loss of total pressure, as represented by $P_{tp} < 1.0$, is caused by the interactions between the two.

The total pressure parameters found during these experiments at Mach 6 and Mach 3 are summarized in Table 3. It can be seen that there is very little difference between the Mach 3, $\theta = 30$ deg values of P_{tp} and the Mach 6, $\theta = 15$ deg values of P_{tp}. This is most likely due to the fact that, although the injectant frontal area, thus blockage, is less for the 15-deg injection case, the freestream Mach number was greater for the $\theta = 15$ deg case, thus offsetting the decreased injectant

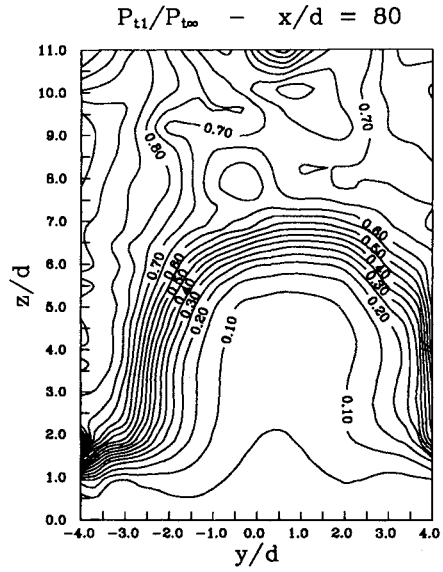

Fig. 15 P_{t1}/P_t: Mach 6, $\theta = 15$ deg, $\beta = 0$ deg, $x/d = 80$.

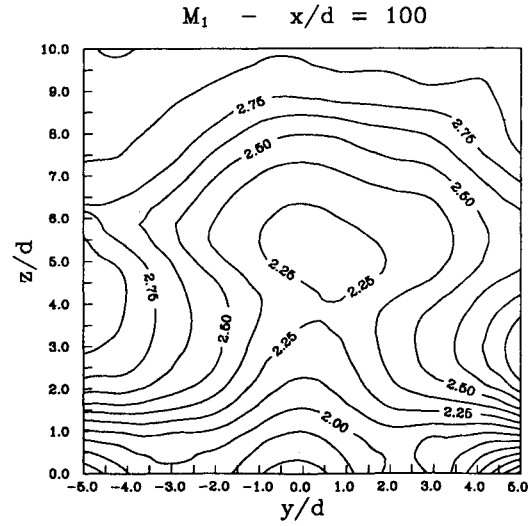

Fig. 16 M_1: Mach 3, $\theta = 30$ deg, $\beta = 0$ deg, $x/d = 100$.

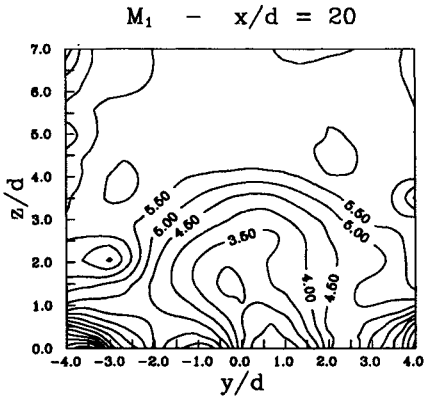

Fig. 17 M_1: **Mach 6, $\theta = 15$ deg, $\beta = 0$ deg, $x/d = 20$.**

frontal area. One can also observe that in the Mach 6, $\theta = 15$ deg experiments, the total pressure parameter was 41% greater for the matched pressure injection case as compared to the 5 × underexpanded case. This was expected because the injection at matched pressure would not plume out as the underexpanded case would, thus the frontal area would be smaller causing less total pressure losses. It can be seen that there were negligible differences in P_{tp} when injector yaw was introduced for each of the three cases.

Figure 15 is a total pressure contour for the case of 5 × underexpanded, Mach 6, $\theta = 15$ deg injection. One can note in this figure that there is a total pressure bucket in that the total pressure in the injectant region is lower than the freestream value would be. This total pressure bucket can be observed to closely match the injectant plume, almost identifying the injectant region, in all injection cases. The size and depth of this total pressure bucket was not found to significantly vary as injector yaw was introduced, as was expected from the nearly identical P_{tp} values.

Two other important flowfield quantities are the local Mach number and flow velocity. Figure 16 presents a Mach number contour from the Virginia Tech Mach 3, $\theta = 30$ deg experiments at $x/d = 100$. One can see that the entire mixing region has remained supersonic. Figure 17 presents a Mach number contour, at $x/d = 20$, found during the Mach 6, $\theta = 15$ deg experiments for the case of 5 × underexpanded injection. The flowfield was found to remain supersonic from $x/d = 20$ to 80. Also observed was that, for all injection cases, the local flowfield velocities were nearly equal to the undisturbed freestream values. In a typical scramjet at high Mach numbers, the injectant velocities would be much lower than the freestream velocity, which could not be simulated in these tests.

Discussion

Helium concentration, pitot pressure, total temperature, and cone-static pressure measurements were taken during the mixing studies conducted in the NASA Langley Mach 6 high Reynolds number tunnel. These studies involved transverse gaseous injection at a downstream angle of 15 deg and injector yaw angles of 0 and − 15 deg for both matched pressure and 5 × underexpanded injectant conditions. These results were compared to $\theta = 30$ deg, 5 × underexpanded helium injection, with yaw angles of 0, − 15, and − 28 deg into a Mach 3 freestream as well as earlier studies by Mays et al.[12] involving helium injection into a Mach 3 freestream at a downstream angle of 15 deg and no injector yaw. From the measurements, helium mass fraction contours, Mach number, local velocity, and total pressure plots were generated. Also calculated were penetration and decay rates of the helium injectant core as well as total pressure losses.

Visual observations were made including 10^{-8} s exposure time shadowgraph pictures and surface flow visualization techniques. The shadowgraphs showed that the injectant contained large eddies, which are significant for injectant-air large-scale mixing. Also seen in the nanoshadowgraphs was that the injectant bow shock showed an apparent unsteadiness, as illustrated by the kinks in the bow shock. This unsteadiness may aid in the injectant mixing. The surface flow experiments proved that large asymmetries, which also may aid in the injectant mixing, are created by low transverse angled injection at a yaw angle to the freestream. From the concentration measurements, one observes that introducing injector yaw is not effective in increasing the maximum concentration decay during the Mach 3, $\theta = 30$ deg experiments. In the Mach 6, $\theta = 15$ deg tests, by coupling injector yaw with the low downstream transverse angle, the maximum concentration decay rate was degraded, and the injectant penetration was decreased. For both the Mach 3 and Mach 6 tests, introducing injector yaw increased the cross-sectional area of the plume. The total entrainment of freestream fluid into the plume was essentially the same with and without yaw. The meanflow data showed that at Mach 3, and at Mach 6, with both matched pressure injection and a 5 × underexpanded jet, the total pressure losses were nearly identical for a yawed jet as compared to an unyawed jet.

The helium concentration measurements at Mach 6 revealed that the core penetration growth rate and the maximum concentration decay rate decreased by 48 and 24%, respectively, as the injectant underexpansion ratio was increased from 1 to 5. The decrease in the concentration decay rate resulted in a 119% increase in the distance for the core to reach the H_2-air stoichiometric ratio $(x/d)_{st}$. These results are contrary to what Mays observed in his Mach 3 experiments where he recorded a 40% increase in the core penetration rate, a 28% increase in the core concentration decay rate, and a 16% decrease in $(x/d)_{st}$, as the injectant underexpansion ratio was increased from 1 to 5.

The thinner boundary-layer thickness in the Mach 6 experiments is believed to be one of the causes for the decrease in the core penetration growth and concentration decay rates. For this reason, an experiment was performed in the Mach 6 facility with a thickened boundary layer to better match the Mach 3 conditions of Mays. These tests showed that with a thicker boundary layer and an injection underexpansion ratio of 5, the injectant core penetration rate increased 68% and the maximum concentration decay rate increased by 5% over the thinner boundary-layer results. This resulted in an $(x/d)_{st}$ for the Mach 6, thickened boundary-layer case being 28% less than the $(x/d)_{st}$ observed during the original boundary-layer case.

In comparing mixing at Mach 3 to Mach 6, for matched pressure injection, the core penetration growth rate and maximum helium concentration decay rate both increased in going from Mach 3 to Mach 6, but a larger distance to H_2-air stoichiometric was observed at Mach 6. For the case of a 5 × underexpanded helium jet, a small decrease in the rates were observed, but a large increase in $(x/d)_{st}$ was found, in going from a Mach 3 to a Mach 6 crossflow. This indicated that there is much less initial mixing at Mach 6 as compared to Mach 3, which results in a much longer scramjet combustor section for both matched pressure and underexpanded injection.

The idea of an effective jet diameter was introduced by use of a jet to freestream mass flow ratio, and when this nondimensionalizing parameter was used, one found that matched pressure injection has a greater penetration growth rate, but less initial penetration. Also observed was that when d_{eff} is used the maximum helium concentration decay rates became essentially identical. In addition, it was seen that matched pressure injection exhibits less initial mixing, as compared to the 5 × underexpanded cases, at both Mach 3 and Mach 6. As expected, the Mach 6 injection cases showed less initial mixing than the Mach 3 experiments.

Acknowledgments

The grant from the Experimental Flow Physics Branch of NASA Langley Research Center with D. Bushnell, S.

Robinson, and M. Walsh as Technical Monitors for this work is gratefully acknowledged.

References

[1]Curran, E., and Stull, F., "The Potential Performance of the Supersonic Combustion Ramjet Engine," Air Force Aero-Propulsion Lab., ASD-TDR-63, Wright-Patterson AFB, OH, 1963, pp. 1, 2.

[2]Swithenbank, J., "Hypersonic Air-Breathing Propulsion," *Progress in Aeronautical Sciences,* Vol. 8, 1967, pp. 229–294.

[3]Waltrup, P., "Liquid-Fueled Supersonic Combustion Ramjets: A Research Perspective," *Journal of Propulsion and Power,* Vol. 3, No. 6, 1986, pp. 515–524.

[4]Schetz, J. A., Thomas, R. H., and Billig, F. S., "Mixing of Transverse Jets and Wall Jets in Supersonic Flow," *Separated Flows and Jets,* edited by V. V. Koslow and A. V. Dovgal, Springer-Verlag, Berlin, 1991.

[5]Rogers, R. C., "A Study of the Mixing of Hydrogen Injected Normal to a Supersonic Airstream," NASA TN L-7386, March 1971.

[6]Rogers, R. C., "Mixing of Hydrogen Injected from Multiple Injectors Normal to a Supersonic Airstream," NASA TN L-7896, Sept. 1971.

[7]Hyde, C. R., Smith, B. R., Schetz, J. A., and Walker, D. A., "Turbulence Measurements for Heated Gas Slot Injection in Supersonic Flow," *AIAA Journal,* Vol. 28, No. 9, 1990, pp. 1605–1614.

[8]Kwok, F., Andrew, P., Ng, W. F., and Schetz, J. A., "Experimental Investigation of a Supersonic Shear Layer with Slot Injection of Helium," AIAA Paper 90-0093, Jan. 1990.

[9]King, P. S., Thomas, R. H., Schetz, J. A., and Billig, F. S., "Combined Tangential-Normal Injection into a Supersonic Flow," *Journal of Propulsion and Power,* Vol 7, No. 3, 1991, pp. 420–430.

[10]McClinton, C. R., "The Effect of Injection Angle of the Interaction Between Sonic Secondary Jets and a Supersonic Free Stream," NASA TN L-8125, Feb. 1972.

[11]Mays, R., Thomas, R., and Schetz, J. A., "Experimental Investigation of Sonic Helium Injection at a Low Downstream Angle into a Supersonic Flow," Virginia Polytechnic Inst. and State Univ., TP VPI-AOE-171, Blacksburg, VA, June 1990.

[12]Johnston, J., and Nishi, M., "Vortex Generator Jets—A Means for Passive and Active Control of Boundary Layer Separation," AIAA Paper 89-0564, Jan. 1989.

[13]Lin, J., Howard, F., and Bushnell, D. M., "Investigation of Several Passive and Active Methods for Turbulent Flow Separation Control," AIAA Paper 90-1598, June 1990.

[14]Schetz, J. A., and Billig, F., "Penetration of Gaseous Jets Injected into a Supersonic Stream," *Journal of Spacecraft and Rockets,* Vol. 3, No. 11, 1966, pp. 1658–1664.

[15]Ng, W. F., Kwok, F., and Ninnemann, T., "A Concentration Probe for the Study of Mixing in Supersonic Flows," AIAA Paper 89-2549, July 1989.

[16]Fuller, E. J., Thomas, R. H., and Schetz, J. A., "Effects of Yaw on Low Angle Injection into a Supersonic Flow," AIAA Paper 91-0014, Jan. 1991.